

DEVELOPMENT OF TUNGSTEN OXIDE HYDRATE PHASES DURING PRECIPITATION-WASHING-RIPENING PROCESS

Cs. Balázi

Research Institute for Technical Physics and Materials Science, Hungarian Academy of Sciences, Hungary, Budapest XII., Konkoly-Thege út 29-33. Mail to: H-1525 Budapest-114, P.O.Box 49

Abstract

Morphological development of tungsten oxide dihydrate, $\text{WO}_3 \cdot 2\text{H}_2\text{O}$ is studied throughout the steps of precipitation of a gel product and the successive washing steps resulting in well defined granular crystalline product. Residual sodium is a persistent contaminant in $\text{WO}_3 \cdot 2\text{H}_2\text{O}$ [4] and the aim of this study is to follow morphological changes against $[\text{Na}^+]$ content and pH of the solution in contact with the solid phase during the washing steps. Ripening periods (the time of contact between $\text{WO}_3 \cdot 2\text{H}_2\text{O}$ and washing solution) were varied and controlled. Considerable changes in morphology of the grains have been registered from the original amorphous to the spindle shaped, polyhedral and rectangular crystallites. Morphology changes have been found to depend on $[\text{Na}^+]$ content and pH of the solution in contact with the solid phase.

1. Introduction

Tungsten oxide hydrates, ($\text{WO}_3 \cdot n\text{H}_2\text{O}$) are important basic materials for the tungsten industry involving the production of carbides, hard metals, power battery and electronic materials. Due to the wide interest in science and

large applicability in modern technology, numerous investigations were made on them. The key properties of these granular materials are morphology, crystalline structure and chemical purity. In present work the preparation route of tungstic oxide dihydrate, $\text{WO}_3 \cdot 2\text{H}_2\text{O}$, ($\text{H}_2\text{WO}_4 \cdot \text{H}_2\text{O}$) is studied. Tungsten oxide dihydrate was proposed for the preparation of stable sols in early papers of colloid chemistry [1, 11, 12]. Several decades later it was applied as basic material of the metastable hexagonal tungsten oxide representing an optimal substance in intercalation chemistry [9, 13]. In Ref. [2] it was stated that the morphology of the end product hexagonal tungsten oxide is determined by the preparation route of the basic material tungsten oxide dihydrate. In a later study it was shown that the preparation route successfully applied for the production of both stable tungsten acid sols and hexagonal tungsten oxide structures implies a considerably high level of persistent background chemical impurities [3]. In this paper the morphological development of tungsten oxide hydrate grains is studied throughout the steps of the multi-step preparation procedure consisting of acidic precipitation and successive washing. It is characteristic of this procedure that the solid grains of tungsten oxide dihydrate are dispersed in changing liquids (at the beginning in the mother liquid and later in dilute washing "waters"). While the solid phase is in

Table 1. Summary of the preparation conditions

Sample	Volume of experiment	Temperature of precipitation	Number of washing	Ripening periods during preparation	Colour and appearance	[Na] in solid, ppm	XRD Guinier
A	1.5x doses	5 °C	8	10 min between each washing step	green-yellow	400	diffuse lines of $\text{WO}_3 \cdot 2\text{H}_2\text{O}$, amorphous
B	3x doses	6 °C	6	15 min between each washing step, 15h after the last washing	yellow	31	$\text{WO}_3 \cdot 2\text{H}_2\text{O}$
C	3x doses	5 °C	6	15 min between each washing step, 15h after the last washing	yellow	58	$\text{WO}_3 \cdot 2\text{H}_2\text{O}$
D/1	1x doses	5 °C	1	17 h between the first and second washing step	green- yellow	4194	diffuse lines of $\text{WO}_3 \cdot 2\text{H}_2\text{O}$
D/2			2	44 h between the second and third washing step	yellow	688	$\text{WO}_3 \cdot 2\text{H}_2\text{O}$
D/3			3	69 h between the third and fourth washing step	yellow	283	$\text{WO}_3 \cdot 2\text{H}_2\text{O}$
D/4			4	10 h between the fourth and fifth washing step	orange	226	$\text{WO}_3 \cdot \text{H}_2\text{O}$
D/5			5	20 h after the fifth washing	yellow	139	$\text{WO}_3 \cdot 2\text{H}_2\text{O}$
F	Freedman, Ref. 6	25 °C	3x in 0.1 N HCl	various	yellow	< 10	$\text{WO}_3 \cdot 2\text{H}_2\text{O}$

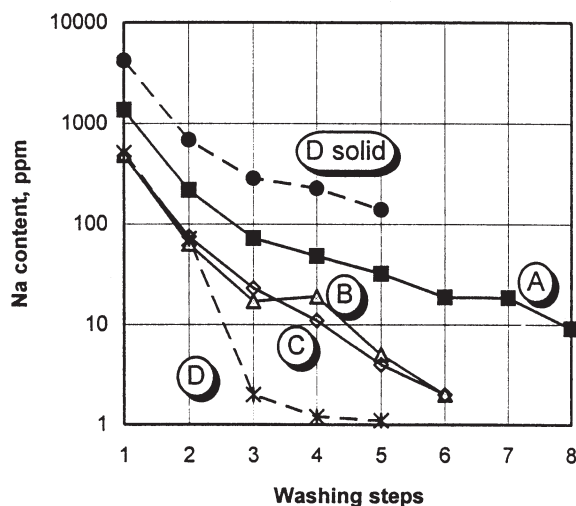


Fig. 1. Observed sodium ion content variation in washing solutions (Samples A, B, C, D) and solid $\text{WO}_3 \cdot 2\text{H}_2\text{O}$ (Sample D) during successive washing steps

contact with the solution morphological changes (ripening) can occur via local dissolution and precipitation or surface diffusion. Morphological changes against $[\text{Na}^+]$ content and pH of the solution in contact with the solid phase have been followed during the washing steps. Preparation experiments have been carried out on various scales; ripening periods have been varied and controlled.

2. Experimental details

Preparation of samples

Tungsten oxide dihydrate ($\text{WO}_3 \cdot 2\text{H}_2\text{O}$) precipitations were obtained according to Zocher's method [4]. Ten and a half grams of $\text{Na}_2\text{WO}_4 \cdot 2\text{H}_2\text{O}$ of analytical grade was dissolved in 150 ml of deionized water and the solution was cooled to 5 °C. To this 75 ml of normal hydrochloric acid solution cooled to the same temperature was added in several doses. Beside this basic dose, preparations scaled up to 1.5 and 3 times were carried out as it is shown in Table 1. The mixture was stirred for 1.5 hr in an ice bath and for 0.5 hr at room temperature (20 °C). After leaving it for about 5 min, then centrifuging the supernatant liquid was removed. Then 200 ml (Sample A) or 600 ml (Samples B, C and D) of water was added to the precipitate and the suspension was stirred 15 min in order to assure the thorough assimilation of the gel. The steps of centrifuging, (5000 r.p.m., 3 - 30 min.), removing the supernatant liquid, and adding 200 or 600 ml of new water were repeated several times. Ripening periods between successive washing steps varied from the minimal processing times of 10-15 min to several tens of hours. At the end of the washing the pH value of the supernatant liquid varied between 3-5, corresponding to the number of washing steps. After each washing step 2g of coagulated gel was removed for chemical, morphological and structural analysis. Sodium content and pH value were determined after each washing step in dried gels and supernatant liquids. Samples ripened for short (10 min), medium (15-70 h) and long time (1 month) were analysed.

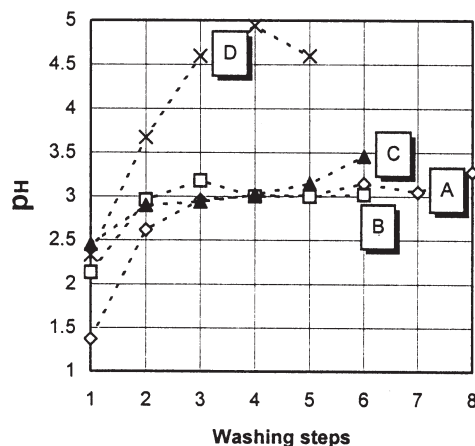


Fig. 2. pH variation of washing solutions (Samples A, B, C, D) during successive washing steps. Resulted phases at the end of washing were crystalline for B, C, D samples and amorphous for A sample

Characterisation of samples

Atomic absorption spectrophotometer (Perkin-Elmer 5000 AAS, flame technique) was chosen as a suitable method for direct determination of small amounts of sodium in the presence of tungsten. X-ray powder patterns were recorded at room temperature in Guinier focussing camera using CuK radiation ($\lambda = 0.154051 \text{ nm}$). Guinier patterns were compared with ASTM powder data files to determine the resulting phases. Infrared absorption spectra were taken by a BOMEM MB-102 FT-IR spectrophotometer, equipped with DTGS detector, at a resolution of 4 cm^{-1} , in KBr pellets, in the range of $400\text{--}4000 \text{ cm}^{-1}$. Morphological analyses were made by JEOL 25 scanning electron microscope.

3. Results

Sodium content and pH value variations during preparations are shown in Fig. 1 and Fig. 2. At the moment of precipitation we obtained amorphous structures. Similar structures and morphologies were found at the end of preparations with short ripening processes (Sample A). During preparations with medium ripening periods (Samples B, C, D) steps of morphological development were observed from amorphous to crystalline spindle shaped $\text{WO}_3 \cdot 2\text{H}_2\text{O}$ grains. Further morphological investigations on long time ripened samples a shape conversion from spindle shape crystals or amorphous grains to rectangular forms.

Rectangular form proved to be the equilibrium shape of $\text{WO}_3 \cdot 2\text{H}_2\text{O}$ grains. Parallel to the morphological changes the structural changes have been studied (Fig. 3, Fig. 4). In agreement with the results of SEM investigations infrared absorption spectra and X-ray diffraction patterns reflected that the first precipitates had amorphous structure (Fig. 5a, Fig. 4a, Table.1). Fig. 5b reveals the appearance of small $\text{WO}_3 \cdot 2\text{H}_2\text{O}$ crystals with morphology that are characteristic for Freedman [6] preparations and represent the first step in morphological development process. Small $\text{WO}_3 \cdot 2\text{H}_2\text{O}$ crystals formation from amorphous state is reflected by infrared spectra (Fig. 4) and XRD mea-

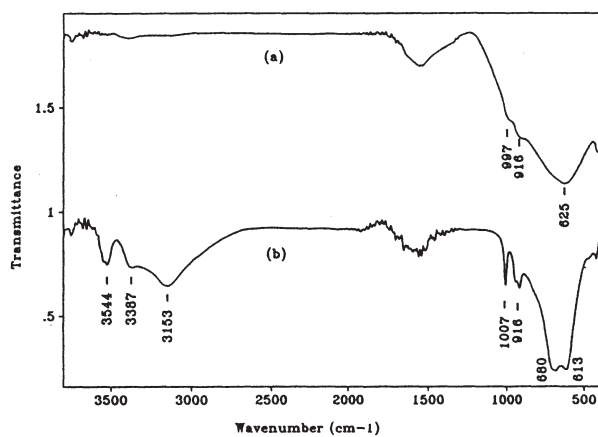


Fig. 3. Evolution with time of infrared spectra (sample A/3), a) slightly ordered $\text{WO}_3 \cdot 2\text{H}_2\text{O}$ gained by a short ripening process, b) crystalline $\text{WO}_3 \cdot 2\text{H}_2\text{O}$ after long time ripening (1 month)

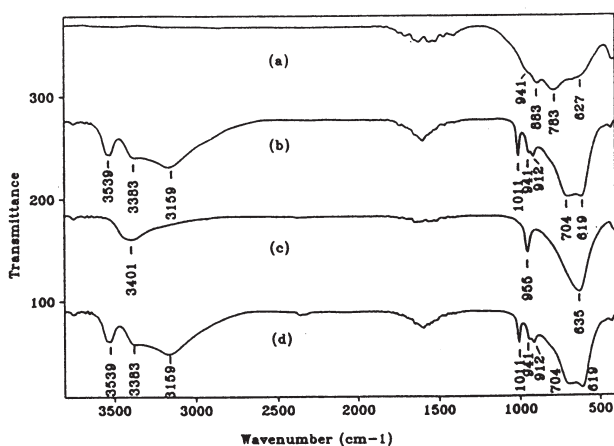


Fig. 4. Evolution with time of infrared spectra (sample D) during successive washing steps and medium ripening periods applied, a) slightly ordered at precipitation moment, b), d) samples D/2, D/5 crystalline $\text{WO}_3 \cdot 2\text{H}_2\text{O}$, c) sample D/4 crystalline $\text{WO}_3 \cdot \text{H}_2\text{O}$

surements too. Fig. 5c is showing the small and large crystal coexistence resulted after second washing procedure. Fig. 5d reflects the typical spindle shaped $\text{WO}_3 \cdot 2\text{H}_2\text{O}$ crystals developed at the end of preparation, reported in Ref. [3, 12, 13]. Long time (1 month) ripened samples are presented in Fig. 5e and Fig. 5f. A step of shape conversion shows Fig. 5e, which can be attributed to a mechanism of crystal growing process (spindle shape platelets — long hexagonal platelets — rectangular platelets). Rectangular shaped $\text{WO}_3 \cdot 2\text{H}_2\text{O}$ grains gained from long time ripening processes are shown in Fig. 5f.

4. Discussion

Experimental results shown above characterise the main features of morphology development throughout the preparation route. During preparations with successive washing steps and medium ripening periods, at the pH = 3.30 value spontaneous set in washing solution we observed a reversible morphological variation from spindle shape crystals to rectangular ones (Fig. 5f). On the other hand we found reversible structural conversions from $\text{WO}_3 \cdot 2\text{H}_2\text{O}$ to $\text{WO}_3 \cdot \text{H}_2\text{O}$ (Fig. 4). These structural and morphological reversible changes indicate (at room tempera-

ture, 20 °C) certain instability characteristic of the tungsten oxide dihydrate gel-solution systems. Morphological investigations on long time ripened samples revealed that exist a pH band from 2.96 to 3.67 in which morphological changes occur, from spindle shaped crystals and amorphous gels to rectangular forms (Fig. 6, Fig. 7). Out of this pH band, at pH < 2.96 and at pH > 3.67 morphological changes had not been found. Furusawa [1] reported a very slow shape conversion to rectangular form with one year ripening period at pH = 2.8 value. Therefore we expect that the pH domain that favored the shape conversion became larger with passing of time. The effect of sodium ion concentration in the solution shows similar features. Amorphous $\text{WO}_3 \cdot 2\text{H}_2\text{O}$ gels with $[\text{Na}^+]$ as high as 4000 ppm for gel and 500 ppm for solution have not shown any tendency for morphology changes, and the shape of very pure ($[\text{Na}^+] < 10$ ppm in solid, $[\text{Na}^+] < 1$ ppm in washing solution) crystalline precipitates have been found stable as well. (Fig. 6, Fig. 7).

These precipitations that resulted very low sodium content samples, prepared by Freedman [6] method

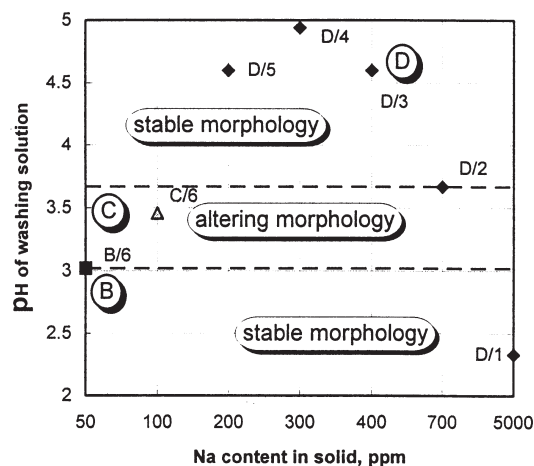


Fig. 6. Long time ripening process effect to $\text{WO}_3 \cdot 2\text{H}_2\text{O}$ grain's morphology: altering morphology (from spindle shape platelets to rectangular platelets, observed at samples B, C, D) between 2.96 and 3.67 pH values, stable morphology at pH < 2.96 and at pH > 3.67

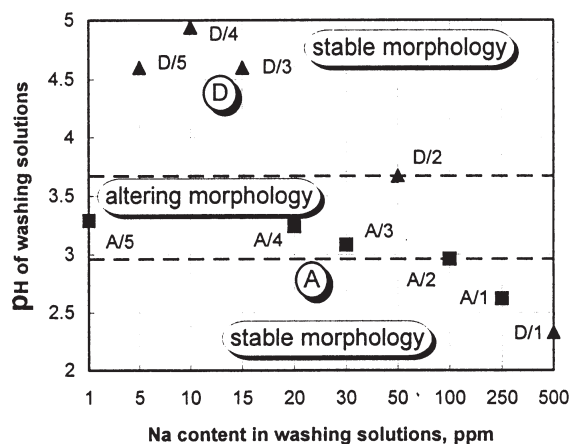


Fig. 7. Long time ripening process effect to $\text{WO}_3 \cdot 2\text{H}_2\text{O}$ grain's morphology: altering morphology (from amorphous grains to rectangular forms at sample A, from spindle shape to rectangular form at sample D) between 2.96 and 3.67 pH values, stable morphology at pH < 2.96 and at pH > 3.67

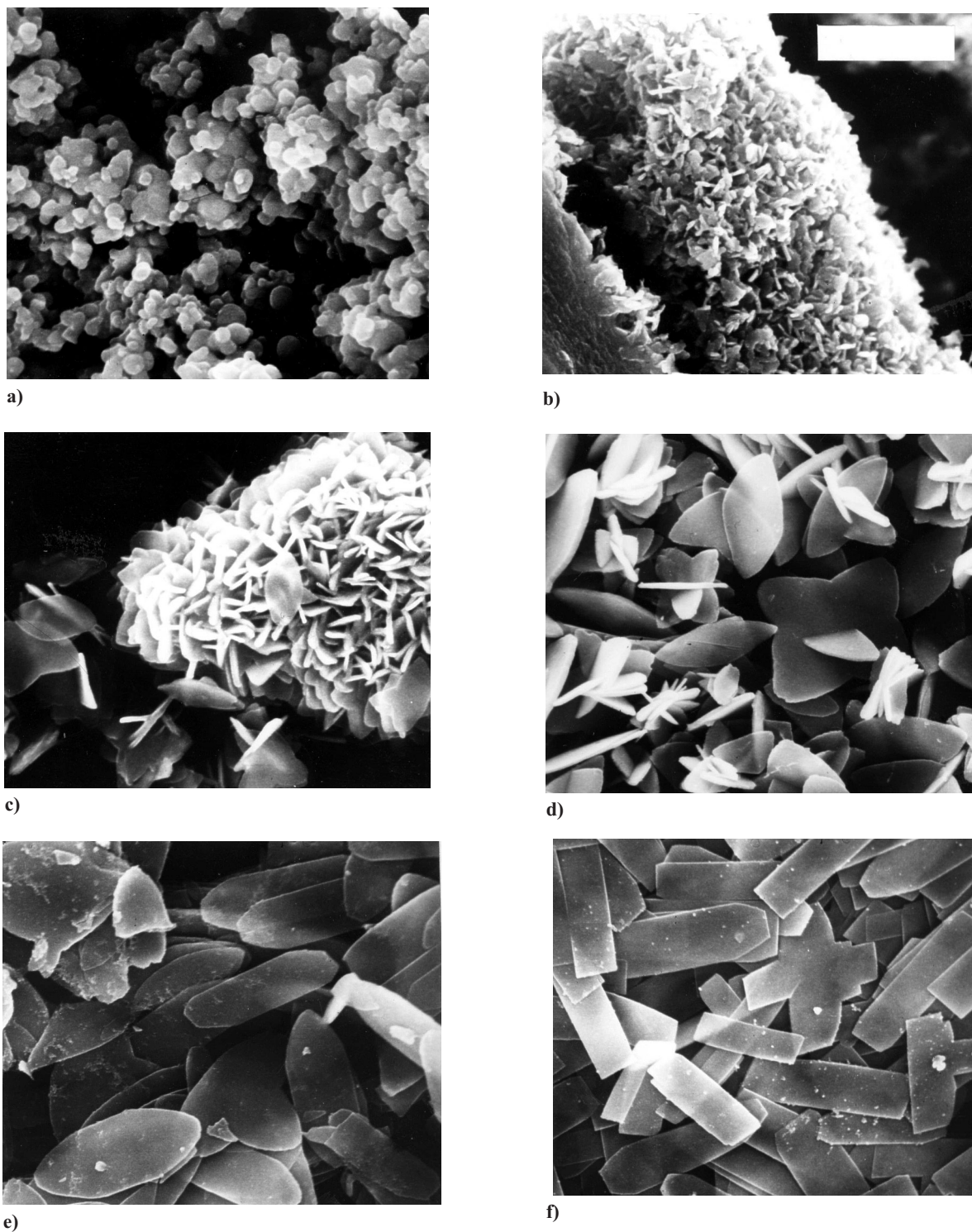


Fig. 5. Scanning electron micrographs presenting the characteristic features of morphological development from amorphous to crystalline spindle shaped $\text{WO}_3 \cdot 2\text{H}_2\text{O}$ (a)-(d), a) Amorphous structure at the moment of precipitation, b) sample D/1 after first washing and 17h ripening small crystallites appeared, c) sample D/2 small and large crystallites coexistence after second washing and 44h ripening, d) sample D/5 spindle shaped $\text{WO}_3 \cdot 2\text{H}_2\text{O}$ crystallites after fifth washing and 20h ripening. Long time ripening period observations (e)-(f), e) Spindle shape platelets of sample C coexisting with hexagonal platelets in the right-upper side of the picture, ripened 1 month in solution with pH 3.46 value, $[\text{Na}^+]$ in solid 58 ppm f) Rectangular platelets of sample D/2 resulting from 1 month ripening, pH of solution 3.67, $[\text{Na}^+]$ in solid 688 ppm, $[\text{Na}^+]$ in solution 71 ppm. Bar: 2.5 μm

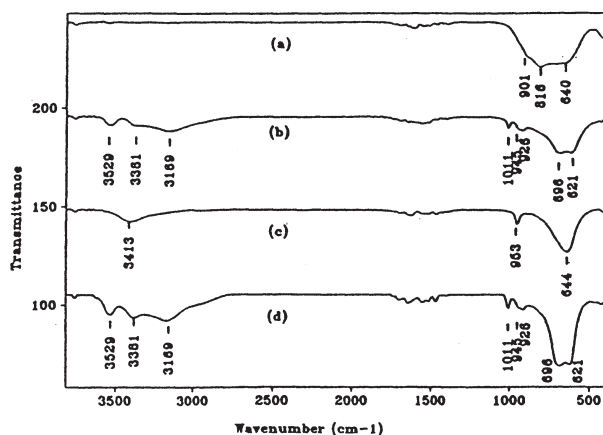


Fig. 8. Evolution with time of infrared spectra (sample D) during long time ripening period (1 month) applied, a) slightly ordered, b), d), samples D/2, D/5 crystalline $\text{WO}_3 \cdot 2\text{H}_2\text{O}$, c) sample D/4 crystalline $\text{WO}_3 \cdot \text{H}_2\text{O}$

(Table.1) are not pointed in figures. Making a comparison between infrared spectra of samples obtained from successive washing steps (Fig. 4) and samples resulted after long time ripening (Fig. 8) only small differences can be found. Crystalline phases ready formed at the steps of preparation have not shown any inclination for structural changes during long time ripening. Comparing the infrared spectra of amorphous samples, little changes are shown at O-W-O bonding vibrations ($600\text{--}700\text{ cm}^{-1}$). The amorphous precipitate of sample D remained with disordered structure after long time ripening (Fig. 4a, Fig. 8a), not the same in the case of sample A. Fig. 3 shows that at certain pH value and $[\text{Na}^+]$ content (Sample A/3) the amorphous -crystalline structural conversion occurred.

5. Conclusion

Morphological development of tungsten oxide hydrate grains was followed throughout the steps of preparation procedure consisting of acidic precipitation and successive washing. Different preparation routes were chosen, ripening periods were varied and controlled. Short ripened samples resulted amorphous structures. By applying medium

ripening periods from amorphous to crystalline forms well-defined morphological changes have been observed (Fig. 5a-5d). During long time ripening periods direct correspondence was found between pH, $[\text{Na}^+]$ content and morphological appearance of $\text{WO}_3 \cdot 2\text{H}_2\text{O}$ grains leading to the rectangular form as the equilibrium shape through a crystal growing mechanism shown in Fig. 5e-5f, Fig. 6, Fig. 7. Infrared absorption measurements proved to be a useful characterisation method for structural investigation of $\text{WO}_3 \cdot 2\text{H}_2\text{O}$ grains exposing all relevant structural transformations that intervened during preparations and ripening processes (Fig. 3, Fig. 4, Fig. 8).

Acknowledgements

The author is grateful to Dr. J.Pfeifer and Dr. K. Vadasdi for many helpful discussions and encouragement. The participation of dr. P. Tekula-Buxbaum, Dr. A.L. Tóth, Dr. B.A. Kiss and J. Mihály in measurements is highly acknowledged. The study was performed within a research program supported by the Hungarian National Research Fund (OTKA, grants no. T 020912 and T015631).

References

1. K. Furusawa, S. Hachisu, *Sci. Light* (Tokio) **15**, 115-130 (1966)
2. B. Gerand, G. Nowogrocki, M. Figlarz, *J. Solid State Chem.*, **38**, 312-320, (1981)
3. J. Pfeifer, Cao Guifang, P.T. Buxbaum, B.A. Kiss, M. Farkas-Jahnke, K. Vadasdi, *J. Solid State Chem.* **119**, 90-97 (1995)
4. H. Zocher, K. Jacobson, *Kolloidchem. Beih.* **28**, (6), 167 (1929)
5. B. Gerand, G. Nowogrocki, J. Guenot, M. Figlarz, *J. Solid State Chem.*, **29**, 429-434 (1979)
6. M.L. Freedman, *J. Amer. Chem. Soc.*, **81**, 3834 (1959)
7. Tsuneo Okubo, *J. Amer. Chem. Soc.*, **109**, 1913-1916 (1987)
8. Hitoshi Suda, Nobuhisa Imai, *J. Colloid. Int. Sci.*, **104**, 204-208 (1985)
9. A. Chemseddine, F. Babonneau, J. Livage, *J. Non. Cryst. Sol.*, **91**, 271-278, (1987)
10. M.F. Daniel, B. Desbat, J.C. Lassegues, B. Gerand, M. Figlarz, **67**, 235-247 (1987)
11. S. Hachisu, K. Furusawa, *Sci. Light*, **12**, 1-8, (1963)
12. S. Hachisu, K. Furusawa, *Sci. Light*, **12**, 157-170, (1963)
13. J. Livage, G. Guzman, *Solid State Ionics*, **84** (1996) 205
14. B. A. Kiss, *Acta Chim. Acad. Scient. Hung.*, **75**, 351-368 (1973)

Table. 2. Experimental and published IR data for $\text{WO}_3 \cdot 2\text{H}_2\text{O}$ and $\text{WO}_3 \cdot \text{H}_2\text{O}$

Attribution	$\text{WO}_3 \cdot 2\text{H}_2\text{O}$		$\text{WO}_3 \cdot 2\text{H}_2\text{O}$		$\text{WO}_3 \cdot \text{H}_2\text{O}$		
	Sample D/2	Sample D/4	Re. 9	Ref. 10	Ref. 9	Ref. 10	Ref. 14
v OH	3539	3401	3530	3530	3400	3390	3400
	3383		3380	3370			
	3159		3170	3160			
δ HOH	1620	1600	1620	1595	1600	1620	1620
	1600	955	1600				
v W-O	1011	955	1010	1007	950	948	949
	941		940	945			
	912		915	918			
v O-W-O	704	635	700	700	640	645	700